



HEALTH SCIENCES

Effect of experimental pulmonary arterial hypertension on renal and bone parameters of rats submitted to resistance exercise training

LEÔNICIO L. SOARES, LUCIANO B. LEITE, MÁIRA O. FREITAS, LUIZ OTÁVIO G. ERVILHA, MAYRA S. PÍCCOLO, ALEXANDRE M.O. PORTES, FILIPE R. DRUMMOND, LEONARDO MATEUS T. DE REZENDE, MARIANA M. NEVES, EMILY C.C. REIS, MIGUEL A. CARNEIRO-JÚNIOR & ANTÔNIO JOSÉ NATALI

Abstract: Pulmonary arterial hypertension (PAH) is characterized by right ventricular failure and diminished cardiac output, potentially leading to renal and bone impairments. In contrast, resistance exercise training (RT) offers cardiovascular and bone health benefits. This study aimed to assess the impacts of stable PAH induced by monocrotaline (MCT) and RT on renal morphometry, as well as bone morphometry and biomechanical properties in male Wistar rats. Four experimental groups, untrained control (UC, n=7), trained control (TC, n=7), untrained hypertensive (UH, n=7), trained hypertensive (TH, n=7), were defined. After the first MCT or saline injection (20 mg/kg), trained rats were submitted to a RT program (i.e., Ladder climbing), 5 times/week. Seven days later the rats received the second MCT or saline dose. After euthanasia, renal and femoral histomorphometry and femoral biomechanical properties were assessed. PAH reduced renal glomerular area and volume, which was prevented by the RT. While PAH did not harm the femoral morphometry, structural and mechanical properties, RT improved the femoral parameters (e.g., length, percentage of trabeculae and bone marrow, ultimate and yield loads). Experimental stable PAH promotes renal but not bone damages, whereas RT prevents renal deteriorations and improves the femoral morphological and biomechanical properties.

Key words: monocrotaline, exercise tolerance, renal morphometry, femoral properties.

INTRODUCTION

Pulmonary arterial hypertension (PAH) is characterized by a progressive increase in pulmonary vascular resistance (i.e., mean pulmonary artery pressure [mPAP] > 25 mmHg), which leads to adverse right ventricular remodeling, dysfunction, and ultimately failure (Taylor et al. 2020). Such pathological condition reduces the blood flow to the entire system, directly contributing to severe renal dysfunctions, such as reduction of the glomerular filtration rate to < 60 mL/min/1.73 m².

Indeed, kidney dysfunction is highly prevalent among PAH patients and poses a significant risk for mortality. There are potential mechanisms to explain the interaction between PAH and kidney disease, including the cardiorenal syndrome and neurohormonal activation (Nickel et al. 2017).

Kidney dysfunction is considered a pivotal factor in the association between vascular calcification and bone demineralization, as renal dysfunction impacts mineral homeostasis (e.g., calcium and phosphate metabolism) and the parathyroid gland activity (Cohen-Solal et al. 2020). Indeed, patients with bone fragility

associated with chronic renal dysfunction exhibit serum parathyroid hormone (PTH) levels below the normal range (Heaf 2001). Furthermore, reduced PTH levels are associated with abnormal values for precursor markers of bone microarchitecture related to bone fragility, such as cross-linked collagen type I peptide, tartrate-resistant acid phosphatase 5B, specific alkaline phosphatase, and procollagen type 1 N-terminal pro-peptide (Pimentel et al. 2021).

Physical exercise, on the other hand, is considered a non-pharmacological therapeutic approach in various pathological conditions, including PAH (Soares et al. 2018). For patients with renal dysfunction, the effects of aerobic and resistance exercises on the kidney function yield inconsistent results. In this context, both aerobic and resistance exercises can either improve the health status of patients with kidney dysfunction or pose a risk factor, potentially increasing proteinuria and renal vasoconstriction, which might strain the system (Poortmans et al. 2001, Bellinghieri et al. 2008, Drew et al. 2013, Qiu et al. 2017, Tadokoro et al. 2022).

Unlike the discordant results regarding the effects of exercise on kidney function, it is well known that mechanical loading generated by physical activities plays a significant role in bone development (Bahia et al. 2020). For instance, exercise training components (e.g., weight bearing, impact, and metabolism) can modify the level of bone turnover through stimulation of osteoblastic and osteoclastic functions (Maimoun & Sultan 2011, Gombos et al. 2016), leading to anabolic effects on bone mineral content and density (Willems et al. 2017). However, some types of short-term exercise may not have significant effects on bone turnover and remodeling (Maimoun & Sultan 2011).

Therefore, considering the elevated prevalence of renal dysfunction in PAH patients and its association with bone fragility, in addition

to the positive impact of physical exercise in such conditions, we decided to employ the model of monocrotaline (MCT)-induced stable PAH in rat to investigate deteriorations in renal and bone morphometry, as well in bone biomechanical properties, and to assess whether resistance training (RT) could mitigate these damages. Our hypothesis is that MCT-induced stable PAH leads to impairments in both renal and bone structural and biomechanical properties, and that RT has the potential to ameliorate these disturbances. Furthermore, we believe these results are relevant for enhancing the understanding of PAH progression and for guiding future studies on the pathological processes of PAH and the application of alternative therapeutic approaches.

MATERIALS AND METHODS

Study design

Male Wistar rats (body weight, ~200 g) were housed in transparent polycarbonate cages, with 4 animals per cage. They were then randomly divided into four groups: untrained control (UC, n = 7), trained control (TC, n = 7), untrained hypertensive (UH, n = 7), and trained hypertensive (TH, n = 7). All animals were kept in a room with a controlled temperature of approximately 22°C, along with ~60% relative humidity. They were maintained under a 12/12 h light/dark cycle and had free access to both water and standard rodent chow. The Ethic Committee for Animal Use at the Federal University of Viçosa approved the experimental protocol (n^o 02/2019) in accordance with the Guide for the Care and Use of Laboratory Animals.

Physical effort tolerance test and resistance exercise training

Rats from all groups (UC, TC, UH, and TH) underwent adaptation to a resistance exercise

training (RT) protocol based on Hornberger & Farrar (2004) over the course of one week. In short, the rats were familiarized with the RT protocol which consisted of climbing a ladder (Dimensions: 1.1 x 0.18 m, 2-cm between steps, 80° of inclination) with devices attached to their tails, but without added weight. Initially, the animals were encouraged to ascend the ladder through a mechanical stimulus applied to their tails to initiate the movement. Once at the top of the ladder, they were allowed to rest in a cage (20 x 20 x 20 cm) for 60 seconds.

After adapting to the RT protocol, all animals underwent a physical effort tolerance test before PAH induction and on the 14th, 21st, and 28th days after the initial MCT or saline injection. This test involved climbing the ladder while carrying an initial load equivalent to 75% of their body weight. Subsequently, the load was incrementally increased by an additional 15% of body weight during subsequent climb, interspersed with a 120 second interval between each ascent, until the animal could no longer climb (Sanches et al. 2014).

After the initial physical effort tolerance test and the first injection of MCT, rats from the TC and TH groups underwent the RT program five times a week for four weeks. The training intensity was set at 55-65% of the carried load in the exercise tolerance test, aligning with recommendations for patients with cardiovascular diseases (Williams et al. 2007). Each exercise training session involved fifteen climbs, separated by a 60-second interval. The training load was adjusted based on subsequent tolerance tests (i.e., on the 14th and 21st days).

Induction of stable pulmonary arterial hypertension

Rats from the UH and TH groups were intraperitoneally injected twice with 20 mg/kg of MCT (Sigma-Aldrich, St. Louis, MO, USA),

solubilized in 1.0 M hydrochloric acid (HCl) and dissolved in a saline solution (140 mM NaCl; pH 7.4) on days 0 and 7 of the experimental period. On the same days, control animals (TC and UC) received an equivalent volume of saline solution (Zhuang et al. 2018). The presence of PAH in animals from the UH and TH groups was characterized by an increased resistance in the pulmonary artery, as indicated by a reduction in the acceleration time to ejection time ratio (AT/ET).

Animals in the UH and TH groups exhibited significantly lower AT/ET values (0.35 ± 0.07 and 0.38 ± 0.08 , respectively) compared to those in the UC and TC groups (0.55 ± 0.06 and 0.55 ± 0.06 , respectively), with $p < 0.05$. Moreover, animals in the UH group demonstrated deteriorated cardiac function, as measured by tricuspid annular plane systolic excursion (TAPSE). They exhibited significantly lower TAPSE values (1.43 ± 0.23 , $p < 0.05$) compared to the UC group (2.06 ± 0.17), TC group (2.35 ± 0.15), and TH group (2.13 ± 0.36).

Euthanasia and murine measurements

Rats from all groups were euthanized by guillotine decapitation on the 30th day after the first injection of MCT or saline. After euthanasia, the heart, ventricles, lungs, soleus, gastrocnemius, kidneys, and femurs were dissected, and their wet weights were obtained using a digital scale (Gehaka - Brasil, model AG 200). Subsequently, these organs were processed for the analyses of interest, as described below. Additionally, an indicator of pathological cardiac hypertrophy, known as Fulton's index, was calculated by dividing the weight of the right ventricle (RV) by the combined weight of the left ventricle and septum.

Histological analyzes

Fragments of the right kidney were submerged in Karnovsky's fixative solution for 24 hours, followed by dehydration in a gradient of crescent ethanol concentrations. Subsequently, the specimens were embedded in glycol methacrylate (Historesin®, Leica, Nussloch, Germany). Three-micrometer thick histological sections were obtained using a microtome (RM 2255, Leica Biosystems, Nussloch, Germany). The sections were then stained with hematoxylin and eosin (H&E) and periodic acid schiff (PAS) for histopathological and stereological evaluation under light microscopy. Digital images from the renal cortex were captured at × 20 magnification using a brightfield microscope (Olympus BX53, Tokyo, Japan) equipped with a digital camera (Olympus DP73, Tokyo, Japan), and were analyzed using the Image-Pro Plus® 4.5 software (Media Cybernetics, Silver Spring, USA). A grid with 266 intersections over a histological field was used to count coincident points over glycogen stained with PAS and then the percentage was calculated. The same technique was used for the stereology of slides stained with H&E. The glomerular area was measured using a specific tool (i.e., manual measurement) using the software Image-pro Plus. The diameter of the glomeruli was measured to determine glomerular volume. Glomerular volume was calculated using the formula $[V = 4/3\pi r^3]$, where r corresponds to the mean value of the glomerular diameter divided by 2 (Sertorio et al. 2019). Seven to fourteen digital images of random histological fields from each animal were used.

For the stereology of the right femur, the proximal epiphyses were fixed in 10% formalin solution in 0.1 M phosphate buffer solution (pH 7.0), for a period of 48 hours, at room temperature, and then were immersed in formic acid descaling solution (12.5%) and sodium citrate (20%) for 30 days. Then, it was dehydrated

in ethanol, clarified in xylol and embedded in liquid paraffin at 60° C in the vertical orientation in relation to the longitudinal axis of the femur (Yoshiki et al. 1983). Blocks were cut into 5 µm-thick sections that were mounted on histological slides and stained with H&E.

To avoid repeated analyzes of the same histological area, in both tissues, the sections were evaluated in semi-series, using one in every 10 sections. Digital images from H&E stained slides were captured using a light microscope (Olympus BX-50, Tokyo, Japan), connected to a digital camera (Olympus Q Color-3, Tokyo, Japan). For the quantification of bone matrix, a grid with 266 intersections was superimposed to the slides, and the intersections in specific tissue were counted and then the percentage was calculated. For all measures, ten random images from each animal were used. All these measurements were performed using Image-pro Plus 4.5 software (Media Cybernetics, Silver Spring, MD, USA).

Biomechanical three-point bending testing

The mechanical properties of the left femur were assessed using a three-point bending test conducted on a materials testing system (MTS, 3367 Dual Column Tabletop Model testing system, Instron, Grove City, PA, USA). The distance between the two support points was tailored to match the length of each bone. A force of 250 N was applied to the bone with a deformation rate of 1 mm/min. Load-deformation curves (Figure 1) were directly obtained from the MTS system and recorded in a computer linked to the testing machine. These data were used for the acquisition and calculation of structural properties: ultimate load, yield load, stiffness and tenacity. The ultimate load is the highest force (N) a specimen can withstand, whereas the yield load represents a force (N) at which a specimen starts to experience permanent

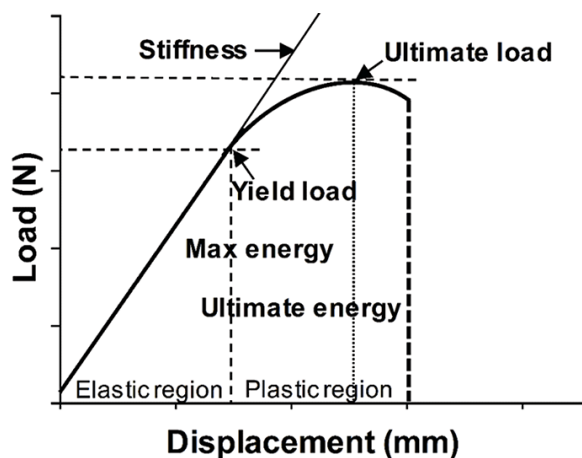


Figure 1. Loading-deformation curve adapted from Turner & Burr (1993). Ultimate load, value of the maximal load; stiffness, slope of the most linear portion of the elastic region; yield load, force at which a specimen starts to experience permanent structural damage; max energy, energy to maximal load, which was the area under the curve up to the point of maximal load; ultimate energy, energy to complete tissue failure, which was the total area under the curve.

structural damage (Akhter et al. 2001). Stiffness was calculated as the slope of the most linear portion of the elastic region of the load-displacement curve (Akhter et al. 2001), while tenacity, which is the amount of energy needed to cause bone fracture during flexion, was calculated by the area under the curve, including elastic and plastic regions (Turner & Burr 1993).

After the analysis of the structural properties, the material properties of the bone were determined by measuring the internal and external diameters of the cross section in each fractured femur. The cross section of the femur was assumed to be a hollow ellipse (Standarts 2003). Then, it was calculated the moment of inertia for irregular cross sections (I) as suggested by Turner & Burr 1993 (Turner & Burr 1993) using the following equation, where a is the width of the cross-sectional area in the mid-lateral direction, b is the width of the cross-sectional area in the anteroposterior direction, and t is the mean cortical bone thickness

(Standarts 2003). The material properties were obtained from these parameters (Akhter et al. 2001).

$$I = \frac{\pi}{64}[a \cdot b^3 - (a - 2 \cdot t) \cdot (b - 2 \cdot t)^3]$$

The following material properties were evaluated: maximum stress (σ); deformation (ϵ); and elastic modulus (E). These parameters were calculated using the following equations, where F is the maximum force applied to the bone, S is the bone stiffness, L is the distance between the two supports, I is the moment of inertia for irregular cross sections, c is the half of b (described in the previous equation); and d is the displacement.

$$\sigma = \frac{F \cdot L \cdot c}{4 \cdot I} \quad \epsilon = \frac{12 \cdot c \cdot d}{L^2} \quad E = \frac{S \cdot L^2}{48 \cdot I}$$

Statistics

The normality of the data was assessed using the Shapiro-Wilk test. Two-way ANOVA followed by Tukey's post hoc test, repeated measures two-way ANOVA followed by Tukey's post hoc test, and paired t-test were employed to identify significant differences between treatments. The specific statistical test used is indicated in tables and figures. Pearson's correlation was utilized to evaluate relationships between the studied variables. Data are presented as mean \pm SD. A significance level of $p < 0.05$ was considered for determining statistically significant differences. All analyses were conducted using GraphPad Prism, version 6.01 (San Diego, CA, USA).

RESULTS

Physical effort tolerance

Regarding the maximum load achieved in the physical exercise tolerance test, no differences were observed between the groups prior to the application of MCT (Table I). However, trained rats (TC and TH) achieved significantly higher maximum load values ($p < 0.05$) on the 14th, 21st,

and 28th days after MCT injection compared to untrained rats (UC and UH). Additionally, the impact of PAH was evident only on the 28th day after induction, where animals in the UH group demonstrated lower maximum load values compared to animals in the UC group

General parameters

Rats injected with MCT exhibited significantly higher values ($p < 0.05$) in right ventricular weights and a greater Fulton's Index (i.e., ventricular weight/left ventricle plus septum weight ratio) compared to their respective controls (Table I). Unfortunately, the RT program was unable to mitigate the pathological hypertrophy observed in hypertensive animals. Similarly, lung weight

and its ratio to body weight displayed elevated values in hypertensive rats when compared to their controls ($p < 0.05$). The RT program utilized in this study also failed to counteract these increases.

Renal histomorphometry

Regarding renal histomorphometry, trained rats (TC and TH) exhibited a higher percentage of glomerulus compared to untrained rats with PAH (UH) (Supplementary Material - Figure S1). In addition, RT led to a reduction in the percentage of extracellular matrix and renal glycogen (Figure 2c and d, respectively), despite the absence of PAH effects on these parameters. There were no differences in the percentage of renal tubules

Table I. Effect of resistance exercise training on physical effort tolerance, whole animal and organ parameters.

| | UC | TC | UH | TH |
|----------------------------------|----------------|------------------|-----------------|---------------------------------|
| <i>Physical effort tolerance</i> | | | | |
| MLPI | 212.30 ± 21.03 | 227.80 ± 25.21 | 223.7 ± 26.56 | 244.00 ± 20.37 |
| ML14 | 296.90 ± 35.59 | 404.50 ± 18.80** | 298.00 ± 36.29 | 453.30 ± 44.62** ^{###} |
| ML21 | 318.00 ± 33.24 | 511.20 ± 56.81** | 265.40 ± 83.80 | 549.30 ± 57.17** ^{###} |
| ML28 | 369.80 ± 34.73 | 639.00 ± 53.02** | 278.50 ± 45.27* | 603.50 ± 83.73** ^{###} |
| <i>Organ parameters</i> | | | | |
| BW final, g | 303.00 ± 22.39 | 315.00 ± 17.86 | 294.30 ± 21.69 | 312.71 ± 08.58 |
| Heart, g | 1.23 ± 0.11 | 1.25 ± 0.15 | 1.30 ± 0.18 | 1.28 ± 0.12 |
| RVW, g | 0.33 ± 0.04 | 0.34 ± 0.05 | 0.42 ± 0.03* | 0.44 ± 0.05* ^{&} |
| LV+SW, g | 0.97 ± 0.09 | 0.96 ± 0.07 | 0.89 ± 0.09 | 1.00 ± 0.06 |
| RVW: LV+SW, g/g | 0.34 ± 0.04 | 0.36 ± 0.04 | 0.47 ± 0.06** | 0.43 ± 0.05* ^{&} |
| RVW: femur length | 0.009 ± 0.001 | 0.010 ± 0.001 | 0.011 ± 0.000* | 0.011 ± 0.0017* |
| LW, g | 1.65 ± 0.28 | 1.84 ± 0.17 | 2.77 ± 0.41** | 2.38 ± 0.33** ^{&} |
| LW: BW, mg/g | 5.46 ± 0.80 | 5.89 ± 0.49 | 9.46 ± 1.67** | 7.87 ± 1.47* ^{&} |
| RKW, g | 1.09 ± 0.05 | 1.08 ± 0.10 | 1.12 ± 0.07 | 1.12 ± 0.08 |
| RKW: BW, mg/g | 3.64 ± 0.20 | 3.47 ± 0.33 | 3.84 ± 0.25 | 3.71 ± 0.29 |
| Soleus, g | 0.13 ± 0.01 | 0.14 ± 0.01 | 0.12 ± 0.00 | 0.15 ± 0.01* [#] |
| Gastrocnemius, g | 1.74 ± 0.17 | 1.82 ± 0.12 | 1.58 ± 0.16 | 1.74 ± 0.23 |

Data are mean ± SD of 7 rats in each group and histomorphometry are of 7–10 images per animal in each group. UC, untrained control; TC, trained control; UH, untrained hypertensive; TH, trained hypertensive. MLPI, maximum load measured prior to monocrotaline (MCT) injection; ML14, maximum load measured 14 days after MCT injection; ML21, maximum load measured 21 days after MCT injection; ML28, maximum load measured 28 days after MCT injection; BW, body weight; RVW, right ventricle weight; LV+SW, left ventricle plus septum weight; LW, lung weight; RKW, right kidney weight. * $P < 0.05$ vs. UC; ** $P < 0.01$ vs. UC; # $P < 0.05$ vs. UH; ## $P < 0.01$ vs. UH; & $P < 0.05$ vs. TC; && $P < 0.01$. TC. Two-way ANOVA followed by the Tukey post hoc test.

were observed among the experimental groups (Figure 2b). The impact of PAH (UH) was evident in the area of the glomerulus and glomerular volume (Figure 2e and f), both of which were lower compared to the control group (UC). Notably, RT (UH) mitigated these changes.

Bone morphometry, structural and material properties and histomorphometry

Rats from the control group that underwent the RT program (TC) exhibited significantly higher femur length values ($p < 0.05$) compared to those in the UC and UH groups (Table II). Similarly, the diaphysis width was significantly greater ($p < 0.05$) in trained animals (TC and TH) in contrast to untrained animals (UC and UH). Concerning the structural and material properties of the femur, PAH did not significantly affect the evaluated parameters ($p > 0.05$) (Table II). However, the RT program increased the ultimate

load and decreased the yield load ($p < 0.05$). Bone material properties remained unaffected by either PAH or RT. Notably, a moderate ($r = 0.599$) and statistically significant ($p = 0.0006$) correlation existed between the maximum load achieved in the final physical effort tolerance test and the maximum sustained load before bone fracture.

Regarding bone histomorphometry, the rats in the trained groups (TC and TH) displayed a higher percentage of bone trabecula and a lower percentage of bone marrow in the femoral proximal epiphysis region compared to the untrained hypertensive animals (UH) (Table II). However, there was no effect of PAH on these parameters (UC vs. UH, $p > 0.05$) (Figure S2, see supplementary material). As for bone histomorphometry, the rats in the trained groups (TC and TH) exhibited higher percentage of bone trabecula and lower percentage of bone

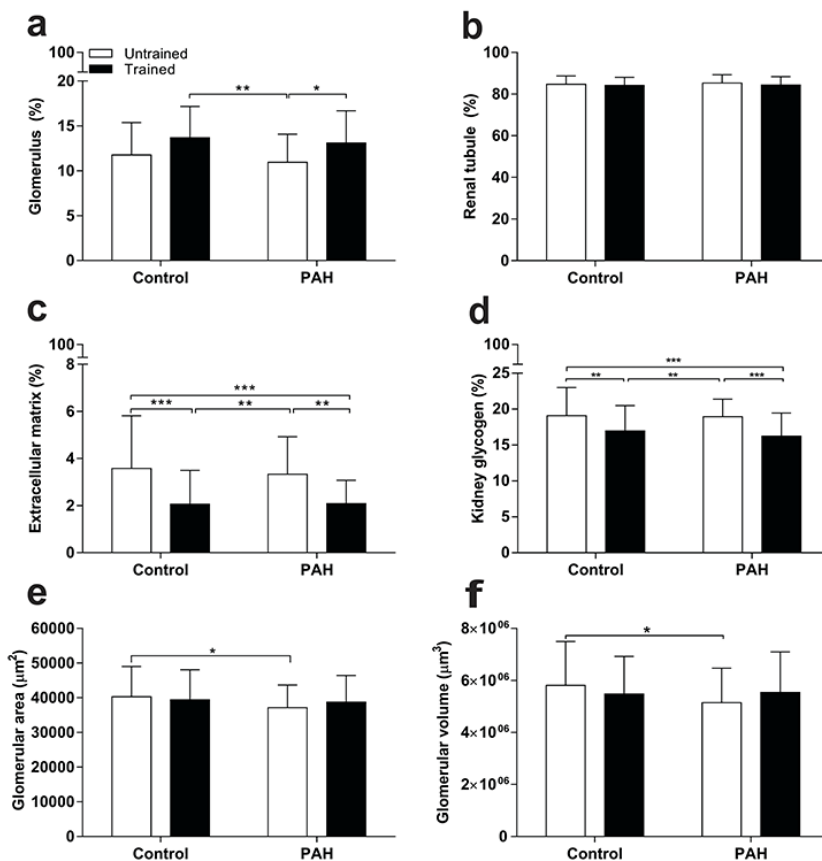


Figure 2. Effect of resistance exercise training on renal histomorphometry. (a) Percentage of glomerulus. (b) Percentage of renal tubules. (c) Percentage of extracellular matrix. (d) Percentage of kidney glycogen. (e) Glomerular area. (f) Glomerular volume. Data are mean \pm SD of 7–14 images per animal in each group ($n = 6-7$ rats in each group). UC, untrained control; TC, trained control; UH, untrained hypertensive; TH, trained hypertensive. * $P < 0.05$; ** $P < 0.01$; *** $P < 0.001$. Two-way ANOVA followed by the Tukey post hoc test.

marrow in the region of the femoral proximal epiphysis, compared to untrained hypertensive animals (UH) (Table II). There was no effect of PAH on these parameters (UC vs. UH, $p > 0.05$) (Figure S2, see supplementary material).

DISCUSSION

We investigated the impact of stable PAH on renal morphometry, bone morphometry, and biomechanical properties using a model of PAH induced by MCT. We also explored whether performing RT during the development of PAH could mitigate these effects. Our findings revealed that while experimental stable PAH led

to renal damage but not to bone impairments, RT prevented renal deteriorations and enhanced both femoral morphological and biomechanical properties.

The primary renal disturbances observed in the studied PAH model included reductions in renal glomerular area and volume. These relatively minor damages are likely triggered by the initiation of cardiorenal disruptions or neurohormonal activations (Nickel et al. 2017). Notably, it is worth mentioning that the use of small MCT doses (i.e., 20 mg/kg) in this experiment, along with the four-week trial period, might have been insufficient for observing more severe renal damage.

Table II. Effect of resistance exercise training on bone morphometry.

| Femur | UC | TC | UH | TH |
|--------------------------------------|----------------|-----------------|----------------|------------------------------|
| <i>Morphometry</i> | | | | |
| Weight, g | 00.93 ± 0.15 | 01.00 ± 00.02 | 00.94 ± 00.05 | 01.00 ± 00.08 |
| Length, mm | 32.68 ± 0.76 | 34.05 ± 01.02** | 32.91 ± 00.42 | 33.34 ± 00.26 |
| PEW, mm | 08.01 ± 0.46 | 08.11 ± 00.20 | 07.92 ± 00.34 | 08.06 ± 00.53 |
| DW, mm | 03.96 ± 0.19 | 04.27 ± 00.14* | 03.92 ± 00.22 | 04.31 ± 00.18** [#] |
| DEW, mm | 05.47 ± 0.34 | 05.32 ± 00.32 | 05.62 ± 0 0.30 | 05.72 ± 00.26 |
| <i>Structural properties</i> | | | | |
| Ultimate load (N) | 65.46 ± 05.51 | 75.53 ± 03.12** | 61.90 ± 07.09 | 73.00 ± 03.79 ^{###} |
| Yield load (N) | 34.94 ± 00.39 | 33.90 ± 00.31** | 36.90 ± 01.76 | 35.41 ± 00.93 ^o |
| Stiffness (N/mm) | 46.27 ± 05.12 | 55.99 ± 10.12 | 49.34 ± 07.30 | 57.15 ± 09.71 |
| Tenacity (N.mm) | 52.24 ± 09.67 | 43.04 ± 13.49 | 61.85 ± 12.12 | 55.89 ± 09.12 |
| <i>Material properties</i> | | | | |
| Ultimate stress (Mpa) | 278.8 ± 38.48 | 239.9 ± 67.38 | 251.1 ± 54.32 | 244.1 ± 55.74 |
| Elastic modulus (N.mm ²) | 4433 ± 491.3 | 4469 ± 909.3 | 4276 ± 1482 | 3945 ± 1290 |
| Strain (mm/mm) | 00.06 ± 00.007 | 00.05 ± 00.007 | 00.06 ± 00.01 | 00.06 ± 00.01 |
| <i>Histomorphometry</i> | | | | |
| Bone trabecula (%) | 15.04 ± 06.15 | 18.05 ± 07.009 | 14.03 ± 05.38 | 17.27 ± 07.48 [#] |
| Bone marrow (%) | 84.96 ± 06.15 | 81.95 ± 07.009 | 85.97 ± 05.38 | 82.73 ± 07.48 [#] |

Data are mean ± SD of 7 rats in each group. UC, untrained control; TC, trained control; UH, untrained hypertensive; TH, trained hypertensive. PEW, Proximal epiphyseal width; DW, Diaphyseal width; DEW, Distal epiphyseal width; Ultimate load, maximum load sustained before fracture; Yield load, load required for bone tissue to begin suffering permanent structural damage; Tenacity, amount of energy needed to cause bone fracture during flexion; Ultimate stress, maximum bone tension; Strain, bone deformation. * $P < 0.05$ vs. UC; ** $P < 0.01$ vs. UC; [#] $P < 0.05$ vs. UH; ^{###} $P < 0.01$ vs. UH; ^o $P < 0.05$ vs. TC; [&] $P < 0.01$. TC. Two-way ANOVA followed by the Tukey post hoc test.

Conversely, the implemented RT program yielded favorable outcomes on several kidney histological parameters (e.g., increase in the percentage of glomeruli, and decrease in the percentage of extracellular matrix and renal glycogen). Renal glomeruli represent the functional units of the kidneys responsible for the entirety of the filtration process and the regulation of blood metabolic waste excretion. These functions are closely intertwined with its essential roles in maintaining general fluid homeostasis, osmoregulation, blood pressure regulation, vitamin D synthesis, bone mineralization, and erythrocyte development (Scott & Quaggin 2015). Conversely, the rate of renal failure progression correlates with the extent of renal fibrosis, which is marked by tubular atrophy, monocyte and macrophage infiltration, fibroblast proliferation and differentiation, and extracellular matrix deposition (Sullivan & Forbes 2019). Renal glycogen, which plays a crucial role in renal homeostasis, becomes a pathological by-product at elevated levels due to excessive production, reabsorption, and utilization of glucose, directly contributing to kidney damage (Sullivan & Forbes 2019). We must emphasize the RT improvements because in situations of possible renal pathologies, such as in diabetes (Sullivan & Forbes 2019), in more advanced stages of hypertension and in heart failure (Torok et al. 2019), RT could be an important tool to minimize renal damages.

Concerning the analyses of bone morphometry and biomechanics, our findings revealed no detrimental effects of the utilized MCT-induced PAH model on the examined parameters. We posit that the reduced oxygen availability resulting from lower cardiac output in PAH patients (Taylor et al. 2020) might not be the primary factor responsible for the loss of bone mass. Other elements, including disease stage, smoking history, corticosteroid use, and age, may

play pivotal roles in determining bone mass and health (Malik et al. 2012). It is noteworthy that the employed PAH model in this study did not induce significant kidney damage, which could potentially influence the mineral homeostasis essential for bone metabolism. Consequently, an extended exposure of rats to a higher dosage of MCT is warranted to comprehensively assess its effects on bone parameters. Additionally, experimental designs employing the MCT PAH model in conjunction with other factors, such as corticosteroid usage, are recommended for further clarification.

Regarding the benefits of RT on bone parameters, we observed that trained rats (TC and TH) exhibited higher ultimate load and yield load compared to the control group. Additionally, both trained groups showed a higher percentage of bone trabeculae and a lower percentage of bone marrow in the femoral proximal epiphysis compared to control rats. It suggests a greater osteoblast activity and bone remodeling in the trained animals. The positive adaptations of long bones to mechanical loading are linked to microfractures within the tissue, which in turn stimulate bone remodeling orchestrated by specialized cells such as osteoblasts, osteoclasts, and osteocytes (Hart et al. 2017, Bahia et al. 2020).

Furthermore, it was observed that the employed RT regimen increased the femoral ultimate load (i.e., the maximum load required to induce fractures) and yield load (i.e., the load needed to initiate permanent structural tissue damage). These adaptations hold significance, as enhancements in bone health are pivotal in various contexts. For instance, in scenarios where the bone system is compromised, such as in more severe cases of PAH (Malik et al. 2012), heart failure (Aluoch et al. 2012), and advanced age (Veldurthy et al. 2016), physical exercise

emerges as a vital strategy to potentially delay or even prevent bone damages.

In the current study, the presence of PAH was characterized by an increase in pulmonary artery resistance. This alteration has been linked to an imbalance between vasoconstrictors (such as endothelin-1 and thromboxane) and vasodilators (including nitric oxide - NO and prostanoids), where vasoconstrictors tend to predominate (Crosswhite & Sun 2014), thus contributing to vascular stiffening and remodeling. Consequently, adverse remodeling of the RV is observed (Ryan et al. 2015). For instance, our hypertensive rats (UH and TH) exhibited a higher Fulton's index in comparison to their respective controls. However, the employed RT program did not avert this occurrence. Furthermore, the rats injected with MCT also displayed increased lung weight, a finding previously reported by others (Natali et al. 2015, Soares et al. 2019). After being metabolized in the liver, MCT is translocated to the pulmonary circulation where it triggers severe pulmonary endothelial damage. This occurs due to an imbalance between vasoconstrictor factors, which outweigh the vasodilator factors, resulting in pathological pulmonary remodeling and, in more advanced stages, pulmonary edema (Zhuang et al. 2018). Regrettably, our RT program did not provide protection against such detrimental remodeling. Nonetheless, it is worth noting that our RT regimen significantly improved physical exertion tolerance in all trained rats.

The increase in the tolerance to physical effort may be explained by the beneficial effects of exercise training in preventing skeletal muscle wasting and dysfunction (Cai et al. 2018) and improving RV cardiac function (Soares et al. 2018). While we have not directly measured the effects of RT on skeletal muscle, it is important to consider the positive impacts of physical training on aspects such as pulmonary

vascular reactivity (Kashimura et al. 1995) and the efficiency of pulmonary gas exchange, which can help prevent hypoxemia during exercise testing (Favret et al. 2006). Taken collectively, these factors contribute to an enhanced cardiac output for the overall system.

Finally, we have chosen to employ a type of low- to moderate-intensity RT (55-65% of a maximum load) and high volume, because of its indication to patients with cardiovascular diseases (Williams et al. 2007). Nevertheless, due to the serious disturbances caused by PAH and the related health risks, any intervention in patients must be cautiously tested under professional supervision.

CONCLUSIONS

We conclude that stable PAH induced by MCT in rats promotes renal but not bone damages, whereas RT prevents renal deteriorations and improves the femoral morphological and biomechanical properties.

Acknowledgments:

LL Soares is thankful to the Coordenação de Aperfeiçoamento de Pessoal de Nível Superior - Brasil (CAPES) for his Ph.D. scholarship. AJ Natali and MM Neves are thankful to the Conselho Nacional de Desenvolvimento Científico e Tecnológico - Brasil (CNPq) for their fellowships. This work was supported in part by the Fundação de Amparo à Pesquisa do Estado de Minas Gerais - Brasil (FAPEMIG), and Conselho Nacional de Desenvolvimento Científico e Tecnológico - Brasil (CNPq). The study supporters were not involved in the study design; collection, analysis, and interpretation of data; the writing of the manuscript; and the decision to submit the manuscript for publication. The authors declare that there are no conflicts of interest.

REFERENCES

AKHTER MP, CULLEN DM, GONG G & RECKER RR. 2001. Bone biomechanical properties in prostaglandin EP1 and EP2 knockout mice. *Bone* 29(2): 121-125.

- ALUOCH AO, JESSEE R, HABAL H, GARCIA-ROSELL M, SHAH R, REED G & CARBONE L. 2012. Heart failure as a risk factor for osteoporosis and fractures. *Current Osteop Rep* 10(4): 258-269.
- BAHIA MT, HECKE MB, MERCURI EGF & PINHEIRO MM. 2020. A bone remodeling model governed by cellular micromechanics and physiologically based pharmacokinetics. *J Mech Behav Biomed Mater* 104: 103657.
- BELLINGHERI G, SAVICA V & SANTORO D. 2008. Renal alterations during exercise. *J Renal Nutr* 18(1): 158-164.
- CAI M, LIU Z, JIA D, FENG R & TIAN Z. 2018. Effects of different types of exercise on skeletal muscle atrophy, antioxidant capacity and growth factors expression following myocardial infarction. *Life Sci* 213: 40-49.
- COHEN-SOLAL M, FUNCK-BRENTANO T & TORRES PU. 2020. Bone fragility in patients with chronic kidney disease. *Endocr Connect* 9(4): R93.
- CROSSWHITE P & SUN Z. 2014. Molecular mechanisms of pulmonary arterial remodeling. *Molecular medicine*, 20: 191-201.
- DREW RC, MULLER MD, BLAHA CA, MAST JL, HEFFERNAN MJ, ESTEP LE & SINOWAY LI. 2013. Renal vasoconstriction is augmented during exercise in patients with peripheral arterial disease. *Physiol Rep* 1(6): e00154.
- FAVRET F, HENDERSON KK, ALLEN J, RICHALET JP & GONZALEZ NC. 2006. Exercise training improves lung gas exchange and attenuates acute hypoxic pulmonary hypertension but does not prevent pulmonary hypertension of prolonged hypoxia. *J Appl Physiol* 100(1): 20-25.
- GOMBOS GC, BAJSZ V, PÉK E, SCHMIDT B, SIÓ E, MOLICS B & BETLEHEM J. 2016. Direct effects of physical training on markers of bone metabolism and serum sclerostin concentrations in older adults with low bone mass. *BMC Musculoskelet Dis* 17(1): 1-8.
- HART NH, NIMPHIUS S, RANTALAINEN T, IRELAND A, SIAFARIKAS A & NEWTON RU. 2017. Mechanical basis of bone strength: influence of bone material, bone structure and muscle action. *J Musculoskelet Neuronal Interact* 17(3): 114.
- HEAF J. 2001. Causes and consequences of adynamic bone disease. *Nephron* 88(2): 97-106.
- HORNBERGER TA & FARRAR RP. 2004. Physiological hypertrophy of the FHL muscle following 8 weeks of progressive resistance exercise in the rat. *Canad J Appl Physiol* 29(1): 16-31.
- KASHIMURA O, SAKAI A & YANAGIDAIRA Y. 1995. Effects of exercise-training on hypoxia and angiotensin II-induced pulmonary vasoconstrictions. *Acta Physiol Scandinav* 155(3): 291-295.
- MAÏMOUN L & SULTAN C. 2011. Effects of physical activity on bone remodeling. *Metabolism* 60(3): 373-388.
- MALIK N, MCCARTHY K & MINAI OA. 2012. Prevalence and significance of decreased bone density in pulmonary arterial hypertension. *Southern Med J* 105(7): 344-349.
- NATALI AJ, FOWLER ED, CALAGHAN SC & WHITE E. 2015. Voluntary exercise delays heart failure onset in rats with pulmonary artery hypertension. *Am J Physiol Heart Circ Physiol* 309(3): H421-H424.
- NICKEL NP, O'LEARY JM, BRITAIN EL, FESSEL JP, ZAMANIAN RT, WEST JD & AUSTIN ED. 2017. Kidney dysfunction in patients with pulmonary arterial hypertension. *Pulmonar Circ* 7(1): 38-54.
- PIMENTEL A, UREÑA-TORRES P, BOVER J, LUIS FERNANDEZ-MARTÍN J & COHEN-SOLAL M. 2021. Bone fragility fractures in CKD patients. *Calcif Tissue Int* 108: 539-550.
- POORTMANS JR, HAGGENMACHER C & VANDERSTRAETEN J. 2001. Postexercise proteinuria in humans and its adrenergic component. *J Sports Med Phys Fit* 41(1): 95.
- QIU Z, ZHENG K, ZHANG H, FENG J, WANG L & ZHOU H. 2017. Physical exercise and patients with chronic renal failure: a meta-analysis. *BioMed Res Int* 2017: 7191826. Doi 10.1155/2017/7191826.
- RYAN JJ, HUSTON J, KUTTY S, HATTON ND, BOWMAN L, TIAN L & ARCHER SL. 2015. Right ventricular adaptation and failure in pulmonary arterial hypertension. *Canadian J Cardiol* 31(4): 391-406.
- SANCHES IC, CONTI, FF, SARTORI M, IRIGOYEN MC & DE ANGELIS K. 2014. Standardization of resistance exercise training: effects in diabetic ovariectomized rats. *Int J Sports Med* 35(04): 323-329.
- SCOTT RP & QUAGGIN SE. 2015. The cell biology of renal filtration. *J Cell Biol* 209(2): 199-210.
- SERTORIO MN, SOUZA ACF, BASTOS DSS, SANTOS FC, ERVILHA LOG, FERNANDES KM & MACHADO-NEVES M. 2019. Arsenic exposure intensifies glycogen nephrosis in diabetic rats. *Environ Sci Pollut Res* 26: 12459-12469.
- SOARES LL, DRUMMOND FR, LAVORATO VN, CARNEIRO-JUNIOR MA & NATALI AJ. 2018. Exercise training and pulmonary arterial hypertension: A review of the cardiac benefits. *Science & Sports* 33(4): 197-206.
- SOARES LL, DRUMMOND FR, REZENDE, LMT, COSTA AJLD, LEAL TF, FIDELIS MR & NATALI AJ. 2019. Voluntary running counteracts right ventricular adverse remodeling and

myocyte contraction impairment in pulmonary arterial hypertension model. *Life Sci* 238: 116974.

SULLIVAN MA & FORBES JM. 2019. Glucose and glycogen in the diabetic kidney: Heroes or villains? *EBioMedicine* 47: 590-597.

STANDARTS ASAE. 2003. Shear and three-point bending test of animal bone. ANSI/ASAE S459 DEC01, USA.

TADOKORO T, TAMURA Y & MOHRI M. 2022. Exercise-induced acute kidney injury. *QJM: Int J Med* 115(1): 47-48.

TAYLOR BJ, SHAPIRO BP & JOHNSON BD. 2020. Exercise intolerance in heart failure: The important role of pulmonary hypertension. *Experiment Physiol* 105(12): 1997-2003.

TOROK RD, AUSTIN SL, BRITT, LK, ABDENUR JE, KISHNANI PS & WECHSLER SB. 2019. Pulmonary arterial hypertension in glycogen storage disease type I. *J Inborn Err Metabol Screen* 5: 1-5. DOI: 10.1177/2326409817707773.

TURNER CH & BURR DB. 1993. Basic biomechanical measurements of bone: a tutorial. *Bone* 14(4): 595-608.

VELDURTHY V, WEI R, OZ L, DHAWAN P, JEON YH & CHRISTAKOS S. 2016. Vitamin D, calcium homeostasis and aging. *Bone Res* 4(1): 1-7.

WILLEMS HM, VAN DEN HEUVEL EG, SCHOEMAKER RJ, KLEIN-NULEND J & BAKKER AD. 2017. Diet and exercise: a match made in bone. *Curr Osteopor Rep* 15: 555-563.

WILLIAMS MA, HASKELL WL, ADES PA, AMSTERDAM EA, BITTNER V, FRANKLIN BA & STEWART KJ. 2007. Resistance exercise in individuals with and without cardiovascular disease: 2007 update: a scientific statement from the American Heart Association Council on Clinical Cardiology and Council on Nutrition, Physical Activity, and Metabolism. *Circulation* 116(5): 572-584. doi: 10.1161/CIRCULATIONAHA.107.185214.

YOSHIKI S, UENO T, AKITA T & YAMANOUCI M. 1983. Improved procedure for histological identification of osteoid matrix in decalcified bone. *Stain Technol* 58(2): 85-89.

ZHUANG W, LIAN G, HUANG B, DU A, XIAO G, GONG J & XIE L. 2018. Pulmonary arterial hypertension induced by a novel method: Twice-intraperitoneal injection of monocrotaline. *Exper Biol Med* 243(12): 995-1003.

SUPPLEMENTARY MATERIAL

Figures S1-S2.

How to cite

SOARES LL ET AL. 2024. Effect of experimental pulmonary arterial hypertension on renal and bone parameters of rats submitted to resistance exercise training. *An Acad Bras Cienc* 96: e20230446. DOI 10.1590/0001-3765202420230446.

Manuscript received on April 16, 2023; accepted for publication on September 1, 2023

LEÔNICIO L. SOARES¹

<https://orcid.org/0000-0001-6852-1230>

LUCIANO B. LEITE¹

<https://orcid.org/0000-0002-3012-1327>

MAÍRA O. FREITAS¹

<https://orcid.org/0000-0001-7520-3097>

LUIZ OTÁVIO G. ERVILHA²

<https://orcid.org/0000-0001-6355-2492>

MAYRA S. PÍCCOLO³

<https://orcid.org/0000-0001-7873-4977>

ALEXANDRE M.O. PORTES⁴

<http://orcid.org/0000-0002-6850-469X>

FILIPE R. DRUMMOND²

<http://orcid.org/0000-0002-6043-9256>

LEONARDO MATEUS T. DE REZENDE¹

<http://orcid.org/0000-0003-3942-3353>

MARIANA M. NEVES²

<http://orcid.org/0000-0002-7416-3529>

EMILY C.C. REIS⁵

<http://orcid.org/0000-0002-9794-6972>

MIGUEL A. CARNEIRO-JÚNIOR¹

<http://orcid.org/0000-0001-5354-7913>

ANTÔNIO JOSÉ NATALI¹

<http://orcid.org/0000-0002-4927-4024>

¹Federal University of Viçosa, Department of Physical Education, Av. PH Rolfs, s/n, University Campus, Center, 36570-900 Viçosa, MG, Brazil

²Federal University of Viçosa, Department of General Biology, Av. PH Rolfs, s/n, University Campus, Center, 36570-900 Viçosa, MG, Brazil

³Federal University of Viçosa, Department of Biochemistry and Molecular Biology, Av. PH Rolfs, s/n, University Campus, Center, 36570-900 Viçosa, MG, Brazil

⁴Federal University of Ouro Preto, Department of Pharmacology, Professor Paulo Magalhães Gomes Street, 122, Bauxita, 35400-000 Ouro Preto, MG, Brazil

⁵Federal University of Viçosa, Department of Veterinary, Av. PH Rolfs, s/n, University Campus, Center, 36570-900 Viçosa, MG, Brazil

Correspondence to: **Luciano Bernardes Leite**

E-mail: luciano.leite@ufv.br

Author contributions

Conceptualization, LLS, MMN and AJN.; methodology, LLS, LBL, LOGE, BRAP, NPP and ECCR; formal analysis, LLS, LBL, LOGE, BRAP, NPP, BAFS, AMOP, FRD, LMTR, TF, EMO; resources, MMN, EMO and AJN; writing, LLS and AJN. All authors have read and agreed to the published version of the manuscript.

